Vibrational Properties of the $LiNbO_3$ *z*-Surfaces

Simone Sanna, Gerhard Berth, Wjatscheslaw Hahn, Alex Widhalm, Artur Zrenner, and Wolf G. Schmidt

***Abstract*—The existence of localized vibrational modes both at the positive and at the negative $LiNbO_3$ (0001) surface is demonstrated by means of first-principles calculations and Raman spectroscopy measurements. First, the phonon modes of the crystal bulk and of the (0001) surface are calculated within the density functional theory. In a second step, the Raman spectra of $LiNbO_3$ bulk and of the two surfaces are measured. The phonon modes localized at the two surfaces are found to be substantially different, and are also found to differ from the bulk modes. The calculated and measured frequencies are in agreement within the error of the method. Raman spectroscopy is shown to be sensitive to differences between bulk and surface and between positive and negative surface. It represents therefore an alternative method to determine the surface polarity, which does not exploit the pyroelectric or piezoelectric properties of the material.**

I. Introduction

The $LiNbO_3$ (0001) surface, commonly known as *Z*-cut, is of particular technological relevance. Indeed, it plays a key role in many emerging applications such as substrate-assisted self-assembly of nanostructures [1] and periodically poled structures [2]. Furthermore, $LiNbO_3$ (0001) [or simply LN(0001)] is attracting attention as a substrate for GaN growth, either for the realization of monolithic optoelectronic amplifiers [3], [4] or as an alternative substrate (to α-Al_2O_3) for the quasi lattice-matched growth of GaN [5]–[8]. The key advantage of this polar surface [the (0001) plane is perpendicular to the spontaneous polarization of the material] is the possibility to reverse the polarization by applying an electric field. Thus, with appropriate ferroelectric domain engineering, it is possible to switch the surface properties. However, to have control over the ferroelectric domains, a deep knowledge of the surface and of the occurring stabilization mechanisms is necessary. The LN(0001) atomic structure has been investigated with the density functional theory (DFT) [9], [10] and by co-axial impact collision ion scattering spectroscopy (CAICISS) [11]. Low-energy electron diffraction (LEED) and reflection high-energy electron diffraction (RHEED) have revealed the absence of any other surface periodicity than the 1×1 [12]. The LN(0001) ionization energy has been determined by UV-photoelectron emission microscopy (PEEM) [13] and its thermal behavior by Auger electron spectroscopy and mass spectrometry [14]. In this work, we investigate the LN(0001) vibrational properties. The study of surface phonons provides valuable insight into the surface structure and other properties specific to the surface region, which often differ from bulk. Furthermore, the knowledge of the surface modes' frequency and dispersion can be used to gain information about surface relaxation, presence of surface defects, and, most of all, surface adsorbates. Driven by the increasing interest regarding quantum dot systems, where the electron-phonon coupling may affect the electrical and optical properties of devices [15], the investigation of the surface phonons has gained a lot of attention. Investigation methods like electron energy loss spectroscopy [16], helium atom scattering [17] Raman, and surface-enhanced Raman spectroscopy (SERS) [18] have been developed or improved. Besides several experimental techniques, there are different *ab initio* theoretical approaches to the investigation of surface dynamics. Among the most successful approaches, we mention the (repeated) slab method in the framework of the DFT [19], [20]. In this approach, particularly suited for the investigation of broad surface phonon phenomena, a supercell (or slab) is created containing relatively thin films of 5 to 50 atomic layers embedded in a vacuum region. The periodic arrangement of the slabs recovers an artificial 3-D periodicity, allowing for the simulation of a semi-infinite solid with parallel surfaces. In our investigation of the vibrational modes of the LN(0001), we combine a theoretical study via supercell approach with Raman measurements. This allows to predict, measure, and classify the surface modes of the investigated system. In a first step, eigenvectors and eigenvalues of the surface phonon modes are calculated from first principles. Surface-localized vibrational modes have been found both at the positive and at the negative LN(0001) face, however, they are qualitatively different. In a second step, we demonstrate that Raman spectroscopy can distinguish between LN bulk and surface and univocally identify the positive and negative LN(0001) surface, and thereby, we concentrate on the detection of the different *A* modes revealed by the calculations. The calculated and measured frequencies are in agreement within the error of the method. The manuscript is organized as follows: in Section II, we briefly describe the experimental setup for the measurement of the Raman spectra, illustrate the slab approach for the calculation of the surface dynamics, and give the computational details of our simulation. In

Manuscript received January 3, 2011; accepted March 27, 2011. The Deutsche Forschungsgemeinschaft (SCHM 1361-12, GRK 1464) is acknowledged for financial support.

S. Sanna and W. G. Schmidt are with the Lehrstuhl für theoretische Physik, Universität Paderborn, Paderborn, Germany (e-mail: simone.sanna@uni-paderborn.de).

G. Berth, W. Hahn, A. Widhalm, and A. Zrenner are with Center for Optoelectronics and Photonics Paderborn and Department Physik, Universität Paderborn, Paderborn, Germany.

Digital Object Identifier 10.1109/TUFFC.2011.2012

0885–3010/$25.00 © 2011 IEEE

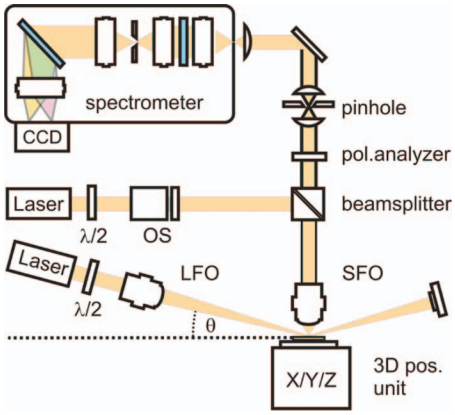

Fig. 1. Schematic representation of the confocal Raman setup.

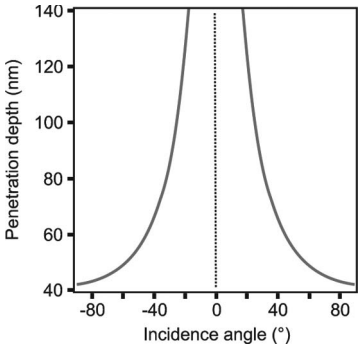

Fig. 2. Penetration depth versus incidence angle according to (1), showing the depth at which the optical power is reduced to a fraction of $1/e$ for the applied wavelength of 532 nm.

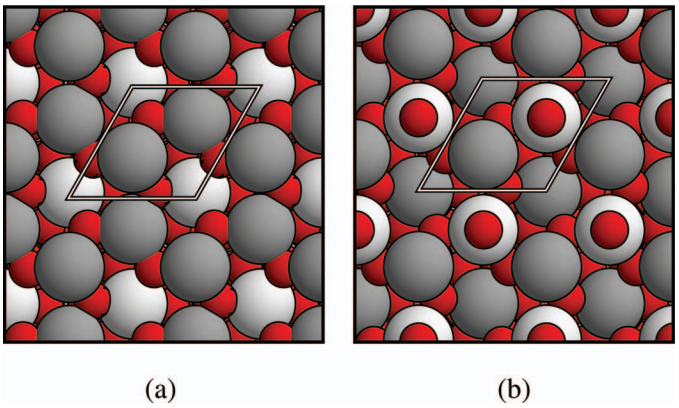

Fig. 3. Top view of the (a) positive and (b) negative LN(0001) surfaces. The big white circles represent Nb atoms, the big gray circles represent Li, and the small red circles are O atoms. The surface unit cell is outlined.

Section III, we show the calculated frequencies for bulk LN and LN(0001) and classify the modes on the basis of their eigenvectors. A few A modes are selected and shown in detail. Raman spectra for LN bulk and for differently polarized LN(0001) surfaces are shown and discussed. Finally, in Section IV, we summarize the main results of our investigation.

II. Methods

Stoichiometric Z-cut lithium niobate (Roditi International Corp. Ltd., London, UK) fabricated as single-domain crystal was utilized. The standard, both sides mirror polished 3-inch (7.62-cm) wafers have been cut into 50-nm-long (X side), 20-nm-wide (Y side), 500-μm-thick (Z side) samples. The absence of differently polarized ferroelectric domains and the surface smoothness have been verified by nonlinear confocal laser scanning microscopy (NCLSM) and atomic force microscopy (AFM), respectively. μ-Raman measurements of the $LiNbO_3$ bulk frequencies were performed by the special confocal setup illustrated in Fig. 1. All of the measurements for the determination of the bulk modes have been accomplished with the 180° scattering configuration.

For the observation of surface phonon modes in the μ-Raman regime, excitation was carried out under grazing incidence (532-nm diode-pumped solid-state laser) instead. In two excitation paths, different objectives were implemented, leading to sample irradiation under a short and a long focus, whereby one path enables the adjustment of different angles of incidence. The penetration depth d_p of the incident laser is defined as the depth at which the intensity is reduced to the fraction $1/e$ of the original value. It can be calculated as a function of the incidence angle α, as

$$d_p = \frac{\lambda}{4\pi \,\mathrm{Im}[\varepsilon - \sin^2 \alpha]}, \tag{1}$$

where λ is the laser wavelength and ε is the sample dielectric function. Therefore, d_p depends explicitly on the laser frequency and implicitly on the frequency dependence of the dielectric function. Using the values reported in [21] for the latter, we obtain the depth profile in Fig. 2. For grazing incidence, calculations yield a penetration depth of about 40 to 45 nm for the adjusted angles.

The scattered light was solely collimated by the short focus objective (OBJ Plan Apo SL 100, NA 0.55, Mitutoyo, Kawasaki, Japan). For detection, a spectrometer (Holospec f/1.8i, Kaiser Optical Systems Inc., Ann Arbor, MI) with adapted CCD-detector (Newton, BI, Andor Technology plc., Belfast, Northern Ireland) was applied. Concerning polarization-dependent measurements, half-wave plates were utilized for defined incident laser polarization; an appropriate analyzer implemented in front of the detection unit specifies the polarization of detection light. Excitation was accomplished in the X- and Y-direction, whereby these are related to the crystallographic axes. Z is parallel to the optical c-axis, X coincides with one of the three equivalent translation vectors of the conventional hexagonal unit cell (see Fig. 3), and Y is chosen to define with X and Z a right-handed orthogonal system. The detailed definition of the X, Y, and Z directions and faces as well as their relationships with the crystal axes, can be found in [9]. Both experiment and theory refer to phonon modes in the center of the Brillouin zone.

We have performed DFT calculations within the generalized gradient approximation (GGA) [22] for exchange and correlation in its PW91 formulation [23] as implemented in the Vienna *ab initio* simulation package (VASP) [24]. Projector-augmented wave (PAW) potentials [25] with projectors up to $l = 3$ for Nb and $l = 2$ for Li and O as well as a plane wave cutoff of 400 eV have been used. The k-space integrations in the electronic structure calculations are performed using shifted Monkhorst-Pack $4 \times 4 \times 1$ meshes [26] equivalent to 24 irreducible points in the two-dimensional Brillouin zone. The dipole corrections described in [27] and [28] have been used to correct the spurious interactions caused by the slab periodic images.

In our work, we accepted the LN(0001) surface structure model proposed in [9] and [10], which we used as basis for the investigation of the vibrational properties. Following this model, which is able to explain the thermal behavior of LN surfaces and other experimental observations [9], [10], the positive surface is -Nb-O_3-Li_2 terminated independently from the growth conditions and the negative surface is O-Li- terminated, as long as the crystal is not grown under extremely O-rich conditions. The atomic structure of the two surfaces is shown in Fig. 3. Our calculations thus refer to the clean surfaces as they should be observed in ultra-high vacuum conditions. Because the measurements were performed at ambient conditions, the appearance of additional adsorbate signals as well as surface phonon frequency shifts caused by the presence of adsorbates cannot be excluded.

The LN(0001) surfaces are simulated by repeated hexagonal slabs with eight trilayers of stoichiometric LN, termination atoms, and a vacuum region of ≈15 Å. The layers are relaxed to minimize the equilibrium forces to less than 0.02 eV/Å. Frozen-phonon calculations [29] without symmetry constraints have been performed up to a depth of 16 and 14 atomic layers within the hexagonal unit cell for the positive and negative surface, respectively. Our approach does not include the long-range electric fields that accompany longitudinal phonons. For this reason, we restrict ourselves to the transverse modes.

Surface phonon modes can have very different dispersion. Surface phonon branches can be completely bound within the bulk phonon dispersion or be localized outside these bands. In the first case, they are called phonon resonances; in the second case, they are referred to as pure surface phonon modes. In the same way, surface phonons can be divided into two groups depending on their origin. Indeed, there are surface modes which can only exist in the surface termination, and surface modes which are the counterpart of bulk vibrations in presence of a surface. The latter take place at energies above or below the corresponding bulk values because of contraction or expansion of the surface layer. Both types of phonons occur in the LN(0001) surface, however we will concentrate in this work only on strongly surface-localized vibrations.

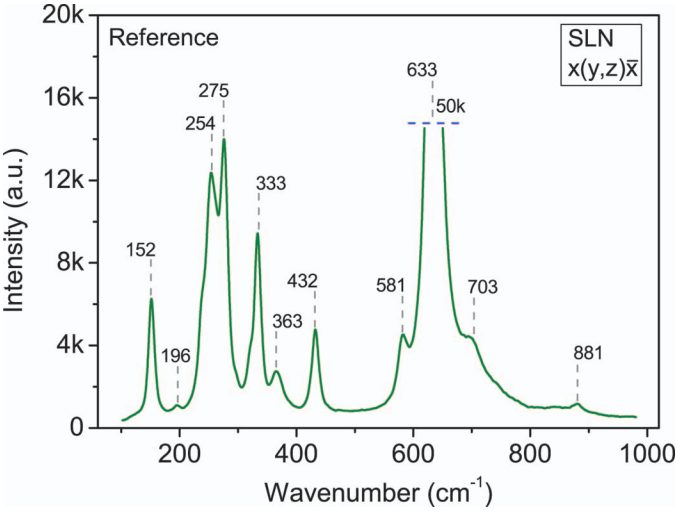

Fig. 4. Raman spectra of bulk $LiNbO_3$. Phonon frequencies (in cm^{-1}) are indicated.

III. Results and Discussion

A. Reference

First, the phonon frequencies of the translational modes in bulk $LiNbO_3$ are measured and calculated. In this way, we have both a check of our approach and a reference spectrum. The Γ-TO modes are split by symmetry into four A_1, five A_2, and nine E modes. The A_2 modes are not Raman active, and will not be discussed in this work. An analysis of the phonon eigenvectors allows classification of the calculated modes as A_1 (if the mode preserves the full crystal symmetry), as A_2 (symmetry preserved, the ions of the same type vibrate in antiphase), and E modes (the crystal symmetry is not preserved, the mode is doubly degenerate). In Fig. 4, we show the Raman spectrum detected for bulk LN with the $X(Y,Z)\bar{X}$ configuration (the Porto notation is used throughout this work). The four Raman active TO A_1 (at 254, 275, 333, and 633 cm^{-1}) and E (at 152, 196, 363, 432, 581, and 693 cm^{-1}) phonon modes are visible and in good agreement with previous measurements [22, and references therein]. An LO mode at 881 cm^{-1} is also visible. Within the DFT calculations, the A_1 modes are found at 240, 286, 353, and 611 cm^{-1}, and the E modes are found at 147, 216, 382, 420, 577, and 667 cm^{-1}. The eigenvectors of the four A_1 modes (labeled by TO1 to TO4) are shown in Fig. 5. TO1 is essentially a z-vibration, with the Nb ions vibrating in antiphase with the oxygen octahedra. TO2 is a z-vibration as well, in which only the Li ions are displaced from the equilibrium positions. TO3 and TO4 essentially involve the oxygen octahedral, and the ionic displacements take place in the xy-plane. Although TO3 consists of an almost rigid rotation of the whole octahedra, in TO4 the displacement pattern is more complex. The ions in one oxygen plane rotate about the trigonal axis as in TO3, whereas the ions of the other plane show a typical breathing movement. The octahedra are thus distorted. The description of the eigen-

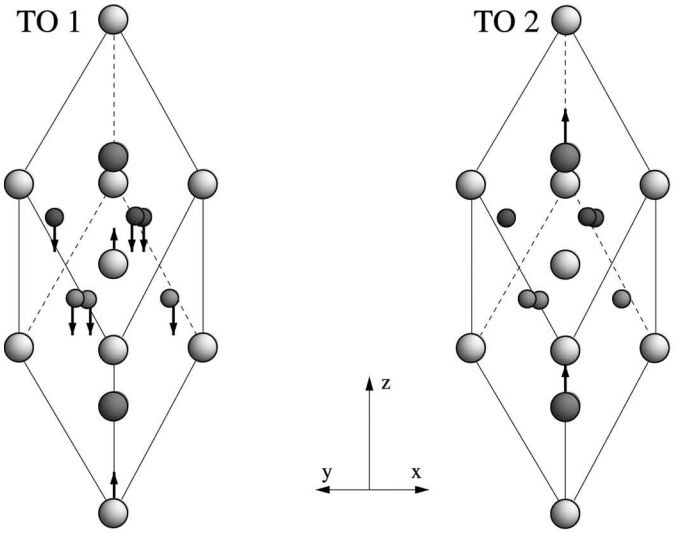

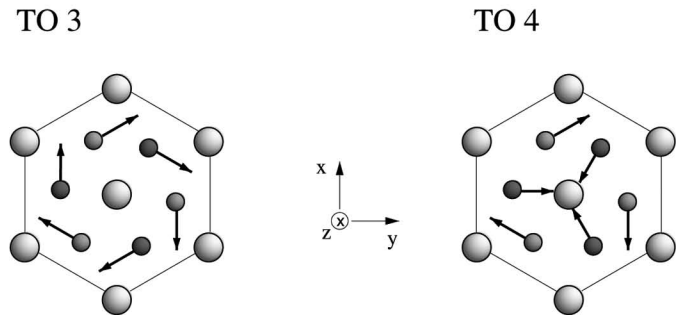

Fig. 5. Schematic representation of the atomic displacements of the four A_1 Γ-TO phonon modes of ferroelectric LN bulk. As in Fig. 3, the big white and gray circles are Nb and Li atoms, the small circles are oxygen atoms.

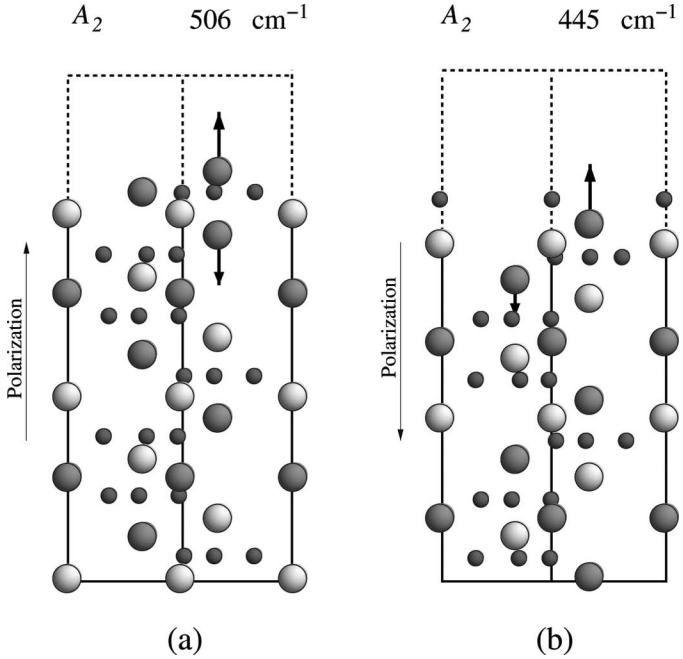

Fig. 6. Schematic representation of the atomic displacements of (a) the phonon mode at 506 cm^{-1} of the positive surface and (b) of a similar phonon mode at 445 cm^{-1} of the negative surface. As in Fig. 3, the big white and gray circles are Nb and Li atoms, the small circles are oxygen atoms.

TABLE I. CALCULATED FREQUENCIES (CM^{-1}) OF THE SURFACE PHONONS AT THE CENTER OF THE SURFACE BRILLOUIN ZONE.

Positive		Negative	
Mode	Freq.	Mode	Freq.
A_1	869	A_1	945
A_1	850	A_1	786
A_2	506	A_1	467
A_1	399	A_2	445
A_1	382	A_1	364
A_1	312	A_1	304
A_2	235	A_1	285
A_1	160	A_2	125

vectors of the E modes is beyond the goals of this study. Within deviations of at most 26, but typically about 10 cm^{-1}, the calculated frequencies match the experimental findings. The accuracy of our calculations is thus comparable to earlier frozen-phonon calculations [21], [30]. Having found a qualitative agreement concerning the bulk modes, we start to investigate the vibrational properties of the (0001) surface.

B. Surface Modes

The zone center phonon modes have been calculated within slab of different thickness to test the substrate dependency of the calculated modes. We observe a slight oscillatory behavior of the mode frequency, which, however, can be considered converged for the slabs with eight atomic tri-layers plus termination atoms. To quantify the localization of the phonons at the surface, we consider for each mode the total atomic displacement in the slab. If the contribution to the total displacement of the termination ions and of the first bulk-like tri-layer is greater than 50%, the mode is considered to be localized at the surface. As in the case of bulk LN, at the Γ point, the optical phonons can be classified according to the irreducible representations of the space group $R3c$ into A_1, A_2, and E modes. In Table I, we report the calculated frequencies of the A surface-localized modes. The phonon frequencies are substantially different and represent a fingerprint of each LN z face. As an example, in Fig. 6 we show the eigenvectors of two similar modes located at the positive surface (at 506 cm^{-1}) and at the negative surface (at 445 cm^{-1}). They are both related to displacements in the Li-sublattice along the z-directions, but have different frequencies because of the different stoichiometry and morphology of the two terminations.

To demonstrate that Raman spectroscopy can be used to univocally identify differently polarized LN surfaces, different spectra have been measured and compared with

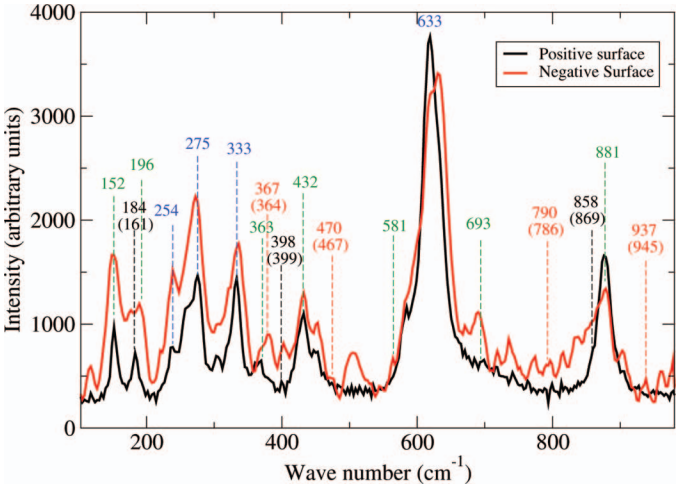

Fig. 7. Raman spectra of the differently polarized LN(0001) surfaces. Green and blue numbers indicate bulk frequencies. Numbers in parentheses are the calculated values.

the calculated frequencies. We used the A_1 modes as a benchmark, because they can be selectively excited in the experiment and because the calculated frequencies of A_1 modes of bulk and surface differ substantially.

In Fig. 7, we show the Raman spectrum measured successively at the two surfaces to reveal the A_1 modes. Even if the spectrum is dominated by the bulk peaks, several features which cannot be traced back to bulk phonon modes appear, thus showing at a first sight that a distinction between bulk and surface is possible. Peaks caused by bulk vibrations have been marked with blue or green labels (references to color refer to the online version of the figure). An analysis of the spectrum of the negative surface reveals peaks at 367, 470, 790, and 937 cm^{-1}, which are predicted by our theoretical model. The calculated values are reported in parenthesis in Fig. 7. Further peaks are present in the spectra, but are not predicted by our model. These can be explained by different effects. First, even if we carry out the measurement within the $X(Y,Z)\bar{X}$ orientation, it cannot be excluded that the sample is irradiated with fractions of not purely Y-polarized light, giving rise to mixed states and peaks not corresponding to A_1 modes. Furthermore, in our theoretical model, we have only considered strongly surface-localized vibrations, whereas our experiment is sensitive to all of the vibrations close to the surface, in particular, bulk vibrations whose frequency is shifted by the presence of the termination.

Concerning the spectrum of the positive surface, we observe that most of the peaks characterizing the spectrum of the negative surface are no longer present. This shows that Raman spectroscopy is able to identify univocally differently polarized LN surfaces. Because the main goal of our investigation is not the classification of each peak, but rather the demonstration of our approach, we do not discuss each mode of the positive surface. The exhaustive classification of the A_1 and E modes of the two surfaces will be the subject of future investigations.

IV. Conclusion

The vibrational properties of the LN(0001) surfaces have been investigated by Raman spectroscopy and DFT calculations. Surface-localized phonon modes have been revealed with both approaches. Calculated and measured surface phonon frequencies are in agreement within the error of the two methods. Raman spectroscopy has been shown to be sensitive to the differences between surface and bulk and between positive and negative LN(0001) surface. It represents, therefore, a non-destructive tool for determining the surface polarity.

Acknowledgments

The calculations were done using grants of computer time from the Paderborn Center for Parallel Computing (PC^2) and the Höchstleistungs-Rechenzentrum Stuttgart (HLRS). The Deutsche Forschungsgemeinschaft (SCHM 1361-12, GRK 1464) is acknowledged for financial support.

References

[1] Y. Yun and E. I. Altman, "Using ferroelectric poling to change adsorption on oxide surfaces," *J. Am. Chem. Soc.*, vol. 129, no. 50, pp. 15684–15689, 2007.

[2] S. Grilli, P. Ferraro, P. De Natale, B. Tiribilli, and M. Vassalli, "Surface nanoscale periodic structures in congruent lithium niobate by domain reversal patterning and differential etching," *Appl. Phys. Lett.*, vol. 87, no. 23, art. no. 233106, 2005.

[3] G. Namkoong, K.-K. Lee, S. M. Madison, W. Henderson, S. E. Ralph, and W. A. Doolittle, "III-nitride integration on ferroelectric materials of lithium niobate by molecular beam epitaxy," *Appl. Phys. Lett.*, vol. 87, no. 17, art. no. 171107, 2005.

[4] K.-K. Lee, G. Namkoong, W. A. Doolittle, M. Losurdo, G. Bruno, and D. H. Jundt, "III-nitride growth and characteristics on ferroelectric materials using plasma-assisted molecular beam epitaxy," *J. Vac. Sci.*, vol. 24, no. 4, pp. 2093–2099, 2006.

[5] S. Sanna and W. G. Schmidt "GaN growth on $LiNbO_3$ (0001)—A first-principles simulation," *Phys. Status Solidi C*, vol. 7, no. 7–8, pp. 2272–2274, 2010.

[6] Y. Tsuchiya, A. Kobayashi, J. Otha, H. Fujioka, and M. Oshima, "GaN heteroepitaxial growth on $LiNbO_3$ (0001) step substrates with AlN buffer layers," *Phys. Status Solidi A*, vol. 202, no. 13, pp. R145–R147, 2005.

[7] S. Sanna and W. G. Schmidt, "GaN/$LiNbO_3$ (0001) interface formation calculated from first-principles," *Appl. Surf. Sci.*, vol. 256, no. 19, pp. 5740–5743, 2010.

[8] A. Ougazzaden, T. Moudakir, T. Aggerstam, G. Orsal, J. P. Salvestrini, S. Gautier, and A. A. Sirenko, "GaN thin films," *Phys. Status Solidi C*, vol. 5, no. 6, pp. 1565–1567, 2009.

[9] S. Sanna and W. G. Schmidt, "Lithium niobate X-cut, Y-cut, and Z-cut surfaces from ab initio theory," *Phys. Rev. B*, vol. 81, no. 21, art. no. 214116, 2010.

[10] S. V. Levchenko and A. M. Rappe, "Influence of ferroelectric polarization on the equilibrium stoichiometry of lithium niobate (0001) surfaces," *Phys. Rev. Lett.*, vol. 100, no. 25, art. no. 256101, 2008.

[11] K. Tabata, T. Choso, and Y. Nagasawa, "The topmost structure of annealed single crystal of $LiNbO_3$," *Surf. Sci.*, vol. 408, no. 1–3, pp. 137–145, 1998.

[12] Y. Yun, M. Li, D. Liao, L. Kampschulte, and E. I. Altman, "Geometric and electronic structure of positively and negatively poled $LiNbO_3$ (0001) surfaces," *Surf. Sci.*, vol. 601, no. 19, pp. 4636–4647, 2007.

[13] W.-C. Yang, B. J. Rodriguez, A. Gruverman, and R. J. Nemanich, "Polarization-dependent electron affinity of $LiNbO_3$ surfaces," *Appl. Phys. Lett.*, vol. 85, no. 12, art. no. 2316, 2004.

[14] A. Ye Lushkin, V. B. Nazarenko, K. N. Pilipchak, V. F. Shnyukov, and A. G. Naumovets, "The impact of annealing and evaporation of $LiNbO_3$ crystals on their surface composition," *J. Phys. D*, vol. 32, no. 1, pp. 9–15, 1999.
[15] Y.-N. Hwang, S.-H. Park, and D. Kim "Size-dependent surface phonon mode of CdSe quantum dots," *Phys. Rev. B*, vol. 59, no. 11, pp. 7285–7288, 1999.
[16] H. Lüth, *Surfaces and Interfaces of Solids*. Berlin, Germany: Springer-Verlag, 1993.
[17] J. G. Skofronick, J. P. Toennies, F. Traeger, and H. Weiss, "Helium atom scattering studies of the structure and vibrations of H_2 physisorbed on MgO(001) single crystals," *Phys. Rev. B*, vol. 67, no. 3, art. no. 035413 2003.
[18] S. Nie and S. R. Emory, "Probing single molecules and single nanoparticles by surface-enhanced Raman scattering," *Science*, vol. 275, no. 5303, pp. 1102–1106, 1997.
[19] G. Benedek, M. Bernasconi, V. Chis, E. Chulkov, P. Echenique, B. Hellsing, and J. Toennies, "Theory of surface phonons at metal surfaces: Recent advances," *J. Phys. Condens. Matter*, vol. 22, no. 8, art. no. 084020, 2010.
[20] F. Bechstedt, *Principles of Surface Physics*. Berlin, Germany: Springer-Verlag, 2003.
[21] W. G. Schmidt, M. Albrecht, S. Wippermann, S. Blankenburg, E. Rauls, and A. Hermann, "$LiNbO_3$ ground- and excited-state properties from first-principles calculations," *Phys. Rev. B*, vol. 77, no. 3, art. no. 035106, 2008.
[22] J. P. Perdew and W. Yue, "Accurate and simple density functional for the electronic exchange energy: Generalized gradient approximation," *Phys. Rev. B*, vol. 33, no. 12, pp. 8800–8802, 1986.
[23] J. P. Perdew, J. A. Chevary, S. H. Vosko, K. A. Jackson, M. R. Pederson, D. J. Singh, and C. Fiolhais, "Atoms, molecules, solids, and surfaces: Applications of the generalized gradient approximation for exchange and correlation," *Phys. Rev. B*, vol. 46, no. 11, pp. 6671–6687, 1992.
[24] G. Kresse and J. Furthmüller, "Efficient iterative schemes for ab initio total-energy calculations using a plane-wave basis set," *Phys. Rev. B*, vol. 54, no. 16, pp. 11169–11186, 1996.
[25] P. E. Blöchl, "Projector augmented-wave method," *Phys. Rev. B*, vol. 50, no. 24, pp. 17953–17979, 1994.
[26] H. J. Monkhorst and J. D. Pack, "Special points for Brillouin-zone integrations," *Phys. Rev. B*, vol. 13, no. 12, pp. 5188–5192, 1976.
[27] J. Neugebauer and M. Scheffler, "Adsorbate-substrate and adsorbate-adsorbate interactions of Na and K adlayers on Al(111)," *Phys. Rev. B*, vol. 46, no. 24, pp. 16067–16080, 1992.
[28] L. Bengtsson, "Dipole correction for surface supercell calculations," *Phys. Rev. B*, vol. 59, no. 19, pp. 12301–12304, 1999.
[29] W. G. Schmidt, F. Bechstedt, and G. P. Srivastava, "III–V(110) surface dynamics from an ab initio frozen-phonon approach," *Phys. Rev. B*, vol. 52, no. 3, pp. 2001–2007, 1995.
[30] A. V. Postnikov, V. Caciuc, and G. Borstel, "Structure optimization and frozen phonons in $LiNbO_3$," *J. Phys. Chem. Solids*, vol. 61, no. 2, pp. 295–299, 2000.

Simone Sanna was born in Cagliari, Italy, in 1977. He graduated in physics in 2003 and received his Ph.D degree in physics in 2007.

Since then, he has been a post-doctoral fellow at the Paderborn University. His research interests are ferroelectrics and point defects.

Gerhard Berth was born in 1971 in Abtsgmünd, Germany. He studied physics in Paderborn, Germany. He graduated in 1999 and received his Ph.D. degree in physics in 2009 from the University of Paderborn. He holds research and teaching positions in Paderborn, Germany. After joining the research training group Micro- and Nanostructures in Optoelectronics and Photonics for two years, he became a post-doctoral research fellow (assistant professor) at the University of Paderborn in 2011. His research interests lie in the physics of optoelectronics and photonics, nonlinear optics, and spectroscopy.

Wjatscheslaw Hahn was born in Nowo-Scharapowka, Russia, on August 9, 1980. He received his B.S. degree in physics from the University of Paderborn, Germany, in 2008 and his M.S. degree in physics in 2011. He works as a research assistant in experimental physics at the University of Paderborn.

Alex Widhalm was born in Burla, Russia, on March 26, 1987. In 2011, he received his B.S. degree in physics from the University of Paderborn, Germany.

Currently, he studies physics in the master's program at the University of Paderborn and has been a student research assistant in experimental physics since 2010. His research interest is Raman spectroscopy

Artur Zrenner was born in 1956. He graduated in physics in München, Germany, in 1983. He received his Ph.D. degree in 1987. Since 2001, he has been professor of experimental physics at Paderborn University. Since 2006, he has been chairman of the Center for Optoelectronics and Photonics Paderborn (CeOPP).

Wolf Gero Schmidt was born in 1968. He studied physics in Jena, Germany. He graduated in physics in 1993, and received his Ph.D. degree in 1997. Since 2006, he has been a full Professor of Theoretical Physics at Paderborn University.

His research interests are the physics and chemistry of surfaces and interfaces, nanoscale science, and computational physics